JOURNAL OF MATERIALS SCIENCE **37** (2002) 3623–3630

The effect of new ferrite content on the tensile fracture behaviour of dual phase steels

M. ERDOGAN*
Materials Division, Metallurgy Education Department, Faculty of Technical Education, Gazi University, 06500, Besevler-Ankara, Turkey
E-mail: merdogan@tef.gazi.edu.tr

The effect of new ferrite present with different volume fractions and morphologies of martensite on microvoids formation and tensile fracture behaviour in dual phase steels has been studied for a steel containing 0.065% C, 1.58% Mn and 0.5% Ni. Fine and coarse dual phase microstructures were obtained from two different starting conditions. Martensite contents were kept constant at ∼18 and ∼25% and new ferrite content was varied by controlled cooling from intercritical annealing temperature of 740, 750 and 785°C. In both fine and coarse dual phase structures microvoids formed at martensite particles, inclusions and martensite-ferrite interfaces in the necked region. Martensite morphology had an influence in determining martensite cracking. Coarse and interconnected martensite distributed along ferrite grain boundaries cracked easily. Martensite cracking was less frequent and the microvoids were smaller in the fine structure than the coarse ones. Microvoid coalescence was the dominant form of fracture in both structures. The specimens with higher new ferrite contents had higher densities of voids. In these samples, voids initiated mostly by decohesion at the interface, and by some examples of fracture of martensite

1. Introduction

The microstructure of dual phase steels consists essentially of relatively hard martensite particles dispersed in a relatively soft and ductile ferrite matrix. This microstructure is obtained by quenching from a temperature at which both ferrite and austenite are present, rapidly enough for a significant fraction of the austenite to transform to martensite. In addition to martensite, the microstructure may contain retained austenite, new or 'epitaxial' ferrite, pearlite and bainite, depending on cooling rate.

Many studies [1–4] have shown that martensite content is dominant in controlling tensile properties and that increasing the amount of martensite decreases ductility. It has been suggested that optimum properties are obtained for dual steels containing ∼20% martensite [1, 5–7]. It has also been shown that, for a constant volume fraction of martensite, a microstructure of finely dispersed martensite yields a better combination of strength and ductility than a coarse microstructure [8–12].

Other factors that have been reported to influence the ductility of dual phase steels include; composition of the martensite, alloy content of the ferrite, retained austenite and the amount of new ferrite [7, 13–17]. Huppi *et al*. [15] showed that at a constant martensite content of 12–14 vol% ductility increased with an increase in the new ferrite content. However the effectiveness of new ferrite present with different volume fractions and morphologies of martensite has not been investigated.

Dual phase steels have been considered for applications which require good formability. For these applications metals may be deformed beyond their uniform strain. The maximum obtainable strain is the combination of uniform strain and nonuniform strain associated with necking. The strain in the neck is controlled by work hardening, work hardening sensitivity and ductile rupture by nucleation, growth and coalescence of microvoids. The distribution of void nucleation sites is dependent on microstructure whereas growth and coalescence of void is controlled by the local stress state at the microvoids.

Fracture is considered the end result of the plastic deformation processes, and may be classified into the two general categories of ductile fracture and brittle fracture. During the process of failure, less energy is expended for brittle fracture than for ductile fracture [18]. Important information about the nature of the fracture can be obtained from microscopic examination of the fracture surface. For this purpose, scanning electron microscopy is generally used, due to the capability of this microscope for large depth of focus [19].

The objective of the present study was to investigate the effect of the new or epitaxial, ferrite present on

*Author to whom all correspondence should be addressed.

microvoid formation and tensile fracture behaviour in dual phase steels containing different volume fractions and morphologies of martensite.

2. Experimental procedure

The composition of the steel used was Fe-0.065C-0.39Si-1.58Mn-0.012P-0.004S-0.55Ni-0.037Al-0.026Nb-0.014Ti-0.03V, wt%. It was supplied in the form of hot rolled plate 18 mm thick. The plate was cut into square rods which were cold rolled to 14×14 mm, normalized at 900°C for 20 min cooled in still air and then swaged to 10.88 mm diameter. The swaged rods were sealed in evacuated quartz capsules and homogenized at 1180°C for 48 h, followed by furnace cooling to room temperature; this removed the slight banding present in the initial plate.

2.1. Heat treatment

In a preliminary investigation to study the dependence of martensite volume fraction on intercritical annealing temperature, 2 mm thick cylindrical slices from homogenized rods were annealed for 20 min in argon at a series of temperatures from 709°C to 868°C and quenched into a 10 wt% brine solution held at −8°C. The martensite volume fraction was determined by point counting on metallographic sections etched in nital. As a result of this preliminary study, three intercritical temperatures of 740, 750, and 785°C were selected for a detailed study of the effect of cooling rate on the development of the dual phase microstructure. These temperatures were chosen in order to specify a series of heat treatments that would vary the new ferrite content at two levels of constant martensite content and two levels of microstructural refinement.

Two levels of refinement of the homogenized microstructure were achieved by:

1. Re-austenitising the homogenized rods at 900°C for 20 min followed by forced air cooling, to produce a microstructure of refined ferrite and pearlite with a small volume fraction of bainitic ferrite and martensite. Dual phase microstructures derived from this initial microstructure were labeled series A.
2. Re-austenitising the homogenized rods at 900°C for 20 min and water quenching to achieve a martensitic microstructure. Dual phase microstructures derived from this initial microstructure were labeled series B.

Specimens of each series were then intercritically heat-treated to obtain dual phase microstructures, with the objective of obtaining two constant levels of martensite with two different dispersions and varying new ferrite contents.

During intercritical annealing of series A specimens, austenite formed in pearlite and martensite and at carbide particles, and partially transformed back to new ferrite and martensite on quenching, depending on cooling rate. The mean linear intercept ferrite grain size was $\sim 10\ \mu$m. In series B specimens, the lath martensite tempered to ferrite and carbide during heating to the intercritical annealing temperature, and austenite formed at carbides in interlath boundaries and between lath packets on a finer scale than in series A specimens. Thus, the martensite volumes formed on quenching from intercritical annealing temperature in series B specimens were smaller and more finely dispersed than in series A specimens, and ferrite grain size was $\sim 6\ \mu$m.

3. Microstructure maps for starting microstructures

In order to control the heat treatment of tensile testpieces in a manner that would provide the required proportions of martensite and new ferrite, it was necessary to construct microstructure maps for the two starting microstructures. Discs 2 mm thick were machined from rods containing series A and series B starting microstructures. A thermocouple was spot welded to the center of one face of each disc, and the discs were intercritically annealed at 740, 750 or 785°C for 20 min in argon. They were then cooled to room temperature in a range of cooling media which resulted in average cooling rates over the first half of the cooling range of about 0.1°C/s–2200°C/s. The proportions of the constituents then present were determined by point counting on etched metallographic sections through the center of the disc. Between 1000 and 2000 points were counted to keep the standard error below 6% of the volume fraction of the minor phases. The etchants used were nital and a hot chromate etch developed by Lawson *et al.* [20] for distinguishing new ferrite.

Figs 1 and 2 illustrate, some examples of the effect of cooling rate on the proportions of phases or constituents present after heat treatment, in the form of microstructure maps, for series A and B starting microstructures and for intercritical annealing temperature of 785°C. The data concerning cooling rates and phase proportions derived from tensile test bars are given in Table I. The microstructure maps allowed heat treatments of tension testpieces to be defined, which would vary the new ferrite content while maintaining a constant martensite content (microstructural compositions are given in volume per cent unless otherwise stated.) For example, in the case of the coarser microstructure, series A intercritical annealing at 785°C and cooling at 95°C/s should result in 25.2% martensite, with 17% new ferrite (Fig. 1) while intercritical

TABLE I Cooling rates and phase proportions in tensile test bars

Specimen code	Cooling rate (°C/s)	Martensite content (vol%)	New ferrite content (vol%)
740A18	18	18.3	6.5
740B18	17	18.4	5.5
750A18	10	18.1	9.5
750B18	6.4	18.1	8.5
785A18	26.6	17.8	25.2
785B18	19.1	18	23.5
740A25	2100	25.8	1.3
740B25	2125	25.1	1.7
750A25	385	25.2	4.4
750B25	350	25.9	3.5
785A25	153	25.2	16.4
785B25	112	25.4	15.3

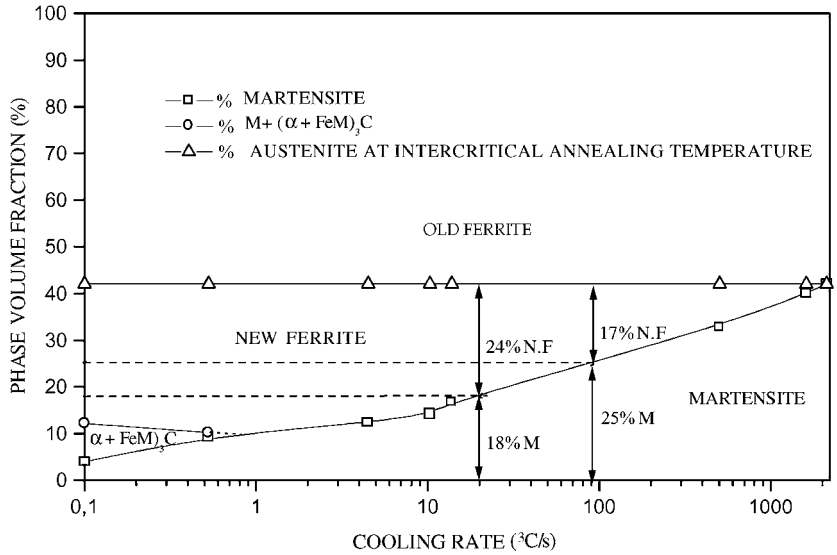

Figure 1 Microstructure map of series A, intercritically annealed at 785°C. (The old ferrite corresponds to presences of original ferrite at interrcritical annealing temperature of 785°C.)

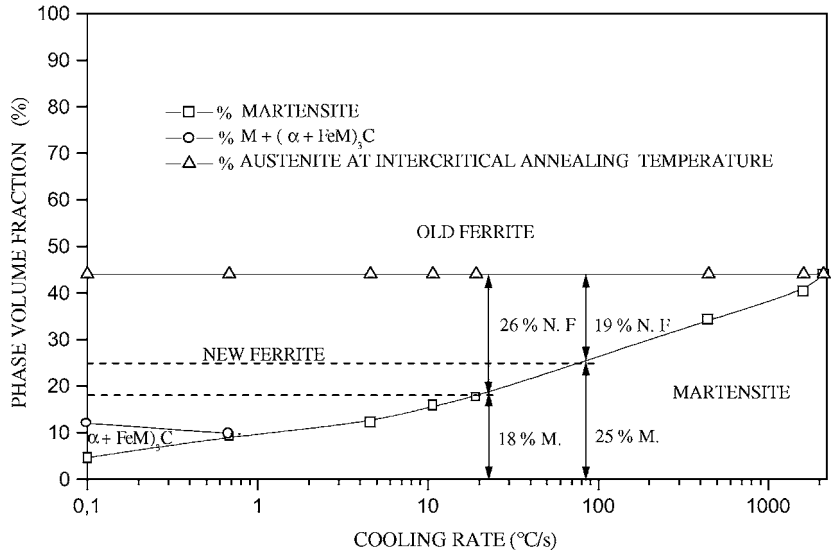

Figure 2 Microstructure map of series B, intercritically annealed at 785°C. (The old ferrite corresponds to presences of original ferrite at interrcritical annealing temperature of 785°C.)

annealing at 740°C and quenching at 2100°C/s should also yield 25.8% martensite but with 1.3% new ferrite (Table I). In Table I, the specimen code includes, first, the intercritical annealing temperature, B = fine starting microstructure, A = coarse starting microstructure and nominal volume fraction of martensite. In another example, in the case of the finer starting microstructure, series B, intercritical annealing at 785°C and cooling at 23°C/s should result in 18% martensite with 26% new ferrite (Fig. 2) while intercritical annealing at 740°C and cooling at 17°C/s should also result in 18.4% martensite but with 5.5% new ferrite (Table I).

A standard X-ray diffraction method [21] was used to examine specimens for the presence of retained austenite. Retained austenite was not detected in most cases, but in a few specimens it was present at the limit of detectability of the method. Small, isolated, nearly spherical particles of retained austenite were observed in some specimens, in quantities too small to be determined by point counting. It was assumed, therefore, that the volume fraction of retained austenite was generally less than 3%, and that variations were unlikely to have a significant effect on mechanical properties.

4. Tensile testing

Testpiece blanks, ~60 mm long, were cut from the 10.88 mm diameter rods which had been homogenized and heat treated to provide the two starting microstructures, A and B. The blanks were intercritically annealed at 740, 750, or 785°C and cooled at controlled rates to obtain either ~18 or 25% martensite with varying new ferrite contents. Surface cooling rates were determined using thermocouples attached to the midpoint of the blank. A tensile testpiece representative of each heat treatment was sectioned longitudinally after testing, and actual phase proportions were determined by point counting. The surface cooling rates and the actual proportions of martensite and new ferrite measured in these specimens are listed in Table I. Because of the larger

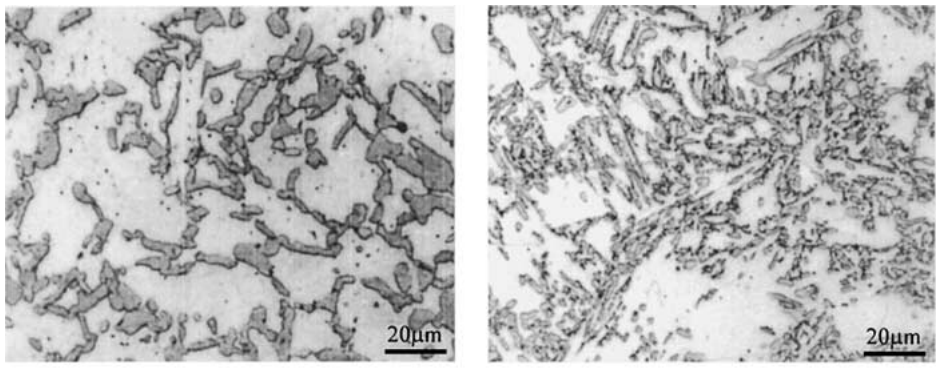

Figure 3 Martensite dispersion in *a* series A, intercritically annealed at 740°C cooled at 2100°C/s to give 25.8% martensite and 1.3% new ferrite and *b* series B intercritically annealed at 740°C cooled at 2125°C/s to give 25.1% martensite and 1.7% new ferrite etched in 2% natal.

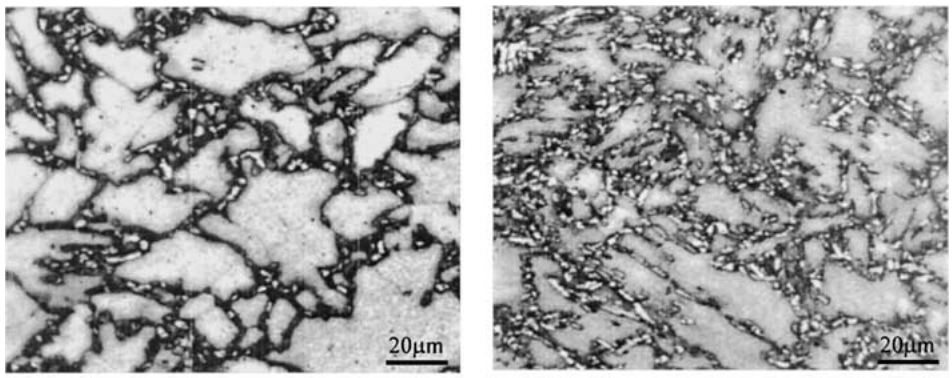

Figure 4 Micrograph of series A (a) and series B (b) specimens. Series A specimen, intercritically annealed at 740°C and cooled at 18°C/s to give 18.3% martensite and 6.5% new ferrite and series B specimen, intercritically annealed at 740°C and cooled at 17°C/s to give 18.4% martensite and 5.5% new ferrite. New ferrite revealed as bright white areas after etching in hot chromate reagent.

thermal mass of the blanks compared with the thin discs used for constructing the microstructure maps, a small amount of new ferrite was present in specimen 740A25 and 740B25 even after cooling at the fastest rates available. The maximum depth of decarburisation was 2 mm, which was removed by machining the testpieces.

The general difference in the martensite dispersion in series A and B specimen is illustrated in Fig. 3. After intercritically annealing the coarser starting microstructure, series A, at 740°C and cooling at 2100°C/s (Fig. 3a), the martensite volume fraction was 25.8% and the new ferrite content was 1.3%; only the martensite and ferrite were distinguished by nital etching in this figure. In the case of the series B specimen intercritically annealed at 740°C and cooling at 2125°C/s (Fig. 3b), the martensite volume fraction was 25.1% and the new ferrite content was 1.7%, and the martensite particles were smaller and more finely dispersed than in series A specimen. Martensite volume fractions were determined on nital-etched metallographic sections. The hot chromate etch did not distinguish well between ferrite and martensite, but revealed new ferrite clearly as shown in Fig. 4. Fig. 4 a and b illustrates series A and B specimens intercritically annealed at 740°C and cooled at 18°C/s, to produce 18.3% martensite with 6.5% new ferrite, and cooled at 17°C/s, to produce 18.4% martensite, with 5.5% new ferrite (revealed by chromate etching as bright, white areas.)

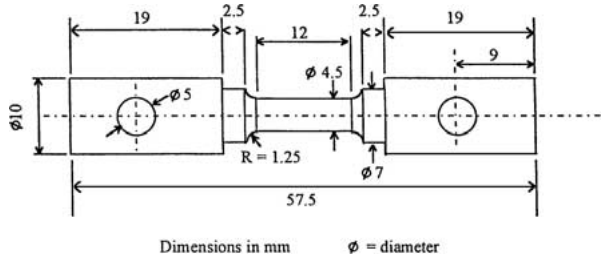

Figure 5 Dimension of specimens (in mm) for tension testing.

Tension testpieces were machined from heat treated blanks to the dimension shown in Fig. 5. This type of testpiece was appropriate for testing in grips which had been specifically designed to allow accurate alignment of the specimen axes with the tensile axis of the testing machine. Longitudinal strain was measured using an extensometer having a gauge length of 10 mm and a nominal strain rate of $1.4 \times 10^{-3}s^{-1}$ and the remainder at $0.7 \times 10^{-3}s^{-1}$; this range of strain rate had no perceptible effect on the stress-strain curves.

After failure, tensile tests specimens were sectioned parallel to the tensile loading direction using a spark (electric discharge machining) machine. The sectioned specimens were ground polished and then etched in 2% nital for metallographic examinatation. These sections were used to observe microstructural change, crack initation and final fracture.

5. Results and discussion

5.1. Tensile fracture of dual-phase steels

Tensile properties of specimens are given in Table II. Tensile fractures were of the ductile cup and cone type. Examples of void formation in necked regions of fractured specimens are shown in Figs 6–11.

Void nucleation was associated with either inclusions (Fig. 6) or the martensite particles. Void nucleation associated with martensite resulted from either decohesion at the ferrite-martensite interface (Fig. 7) or from the separation of adjacent particles (Fig. 8) and localized deformation of martensite particles.

TABLE II The tensile properties of series A and B specimens with different volume fraction and morphology of martensite

Specimen code	Average martensite particle size (μm)	True uniform strain (%)	Max. true stress (MPa)	Total elongation (%)
740A18	2.13	14.2	693.0	39.7
740B18	1.38	14.2	779.3	43.5
750A18	2.45	15.8	701.4	35.3
750B18	1.34	15.4	750.5	43.1
785A18	2.02	17.9	697.1	39.4
785B18	1.38	17.7	730.7	48.5
740A25	3.26	15.7	805.9	31.4
740B25	2.18	12.4	842.3	31.3
750A25	3.26	15.8	799.4	31.7
750B25	2.37	14.2	812.5	32.7
785A25	3.16	14.2	774.4	33.5
785B25	2.16	17.9	767.9	38.9

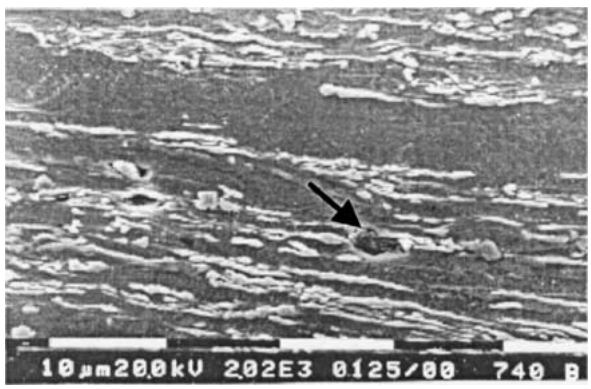

Figure 6 Microvoid formation near the fracture surface for 740B18.

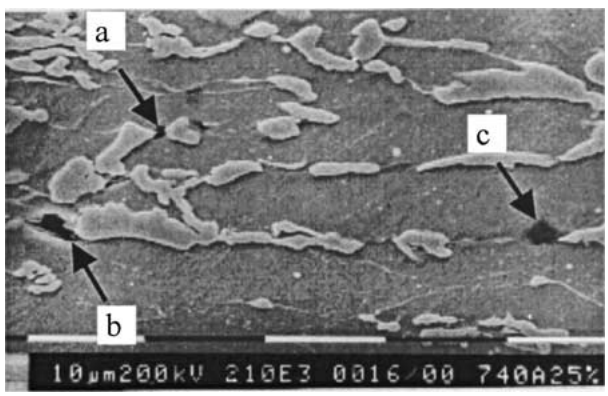

Figure 7 Martensite cracking (arrow a) and microvoid formation within the necked region (arrow b and c) for 740A25.

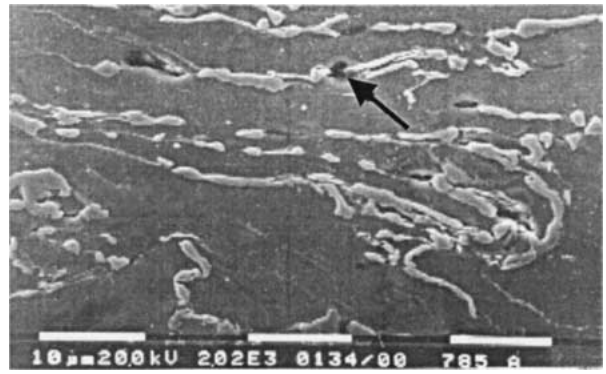

Figure 8 Microvoid formation at martensite particles within the necked region for 785A18.

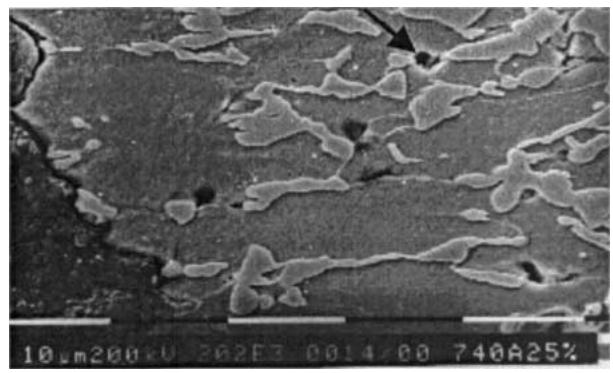

Figure 9 Microvoid formation near the fracture surface for 740A25.

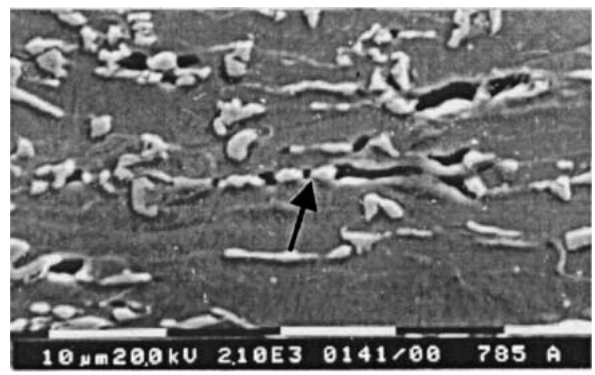

Figure 10 The microvoids propogation parallel to strain direction near the fracture surface for 785A18.

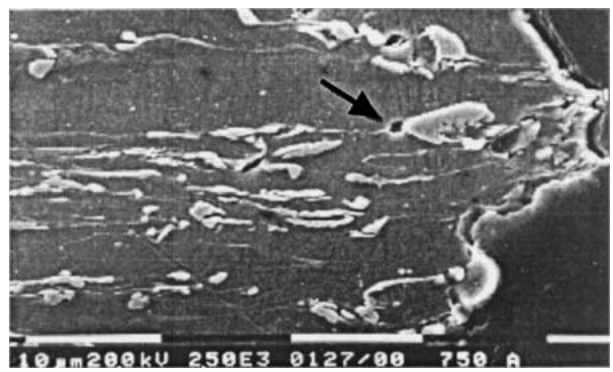

Figure 11 The alignment of martensite and ferrite near the fracture surface for specimen 740A18.

When the strain became severe, a void opened up between two particles (Fig. 9). Similarly, locally deformed martensite particles, having cracked, also separated (Fig. 10). Microvoids formed at α-M interfaces

propagated into ferrite in the direction of straining (Fig. 11).

The degree of martensite connectivity could be an important factor in determining crack initiation at martensite particles. In the coarse microstructure, a martensite particle aligned along a ferrite grain boundary could crack easily (Fig. 7 arrow a).

It was observed from SEM micrographs that the microvoid density in Series A and B increased near the fracture surface. A similar observation was made by Strenbrunner *et al*. [22]. High density of microvoids near to the fracture surface is generally associated with high true strain in this region. During tensile testing, failure of dual phase steels has been attributed to void formation, which has been observed primarily within the necked region at high local strain [23].

It was also observed that martensite cracking in Series B specimens was less frequent and voids were always smaller, relative to Series A specimens. This is due to the reduced martensite connectivity and the smaller particle size of martensite in Series B. Generally, strengths of Series B specimens were also higher than those Series A specimens (Table II). The greater tensile and yield strength of series B may be attributed to different particle size and spacing. Thomas [24] suggested that a finely dispersed, hard second phase in a soft matrix should offer more effective barriers to motion of dislocations and provides more effective composite strengthening for a fixed MVF.

The specimens with higher new ferrite contents had higher densities of voids (Fig. 10). In these samples, voids resulted mostly by decohesion at the interface, with some examples of fracture of martensite. This may be attributable to the presence of the higher content of softer, new ferrite.

Huppi *et al*. [15] showed that ductility was enhanced with increasing volume fraction of new ferrite. This is substantiated in the present work. The present work also indicated that new ferrite in the fine microstructure was much more effective than those in a coarse microstructure. Huppi *et al*. explained the reason for improvement in ductility by referring to Geib *et al*.'s [25] TEM evidence of the absence of precipitation in new ferrite. Gaib *et al*. showed that a precipitate structure developed in the old ferrite of Nb-microalloyed steel during intercritical annealing. Precipitate-free new ferrite formed during cooling. The precipitate-free new ferrite was expected to have a higher ductility and lower strength than the old ferrite .

In dual phase steels, microvoids nucleate at nonmetallic inclusions [26–29] or martensite particles [22, 23, 30]. Nucleation of voids at martensite particles starts either by decohesion at the ferrite-martensite interface, or brittle fracture of the martensite particles [22, 30]. The void density was reported to increase towards the fracture surface and the void density was higher in samples which exhibited localised necking [29, 31].

He *et al* . [32], studied fracture mechanisms in coarse and fine Fe-Mn-C dual phase microstructures having 17% martensite. They observed that in the coarse structure the initial void formation was due to cracking of the martensite at very low strain levels, which was followed by decohesion at ferrite-martensite interfaces. The decohesion type of voids were more frequent in the necked region.

Speich and Miller [30] observed that in dual phase microstructures having low volume fraction and high carbon content of martensite, martensite particles cracked or decohered more easily than those martensite particles in microstructures having high volume fraction and low carbon content of martensite. Therefore, the ductility should decrease with increasing carbon content in the martensite.

Figs 6, 10 and 11 show the elongated microstructure near the fracture surface in Series A and B. From these micrographs, it is clear that ferrite deformed plastically and martensite reorientated.parallel to strain direction during necking.

Microvoid coalescence seems to be the dominant form of fracture. The dimple depressions in the fracture surface is evidence of ductile fracture [Figs 12–15). These figures also show some deep, large cusps. Formation of very deep cusps may be attributed to martensite or inclusion cracking. The wavy nature along the wall of these cusps show the deformation of the surrounding ferrite during the final period of straining up to fracture (Figs 12–14). The fracture surface of specimen 740A25, which had the lowest new ferrite content, showed mostly ductile dimples (Fig. 15) with a few cleavage facets.

Ductile fracture is characterised by dimple-like depressions in the fracture surface that may be equiaxed

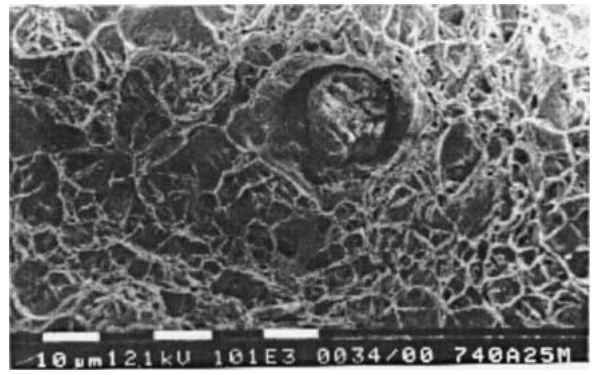

Figure 12 Fracture surface of specimen with ductile dimples and big inclusions in 740A25.

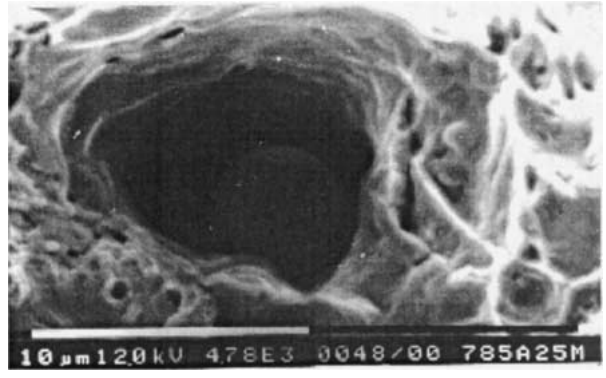

Figure 13 Fracture surface of specimen 785A25 showing big holes with inclusion and the wavy nature along the hole.

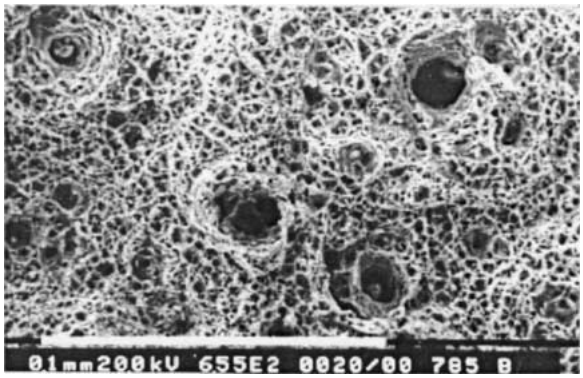

Figure 14 Fracture surface of specimen 785B18 showing ductile dimples and big holes with inclusions.

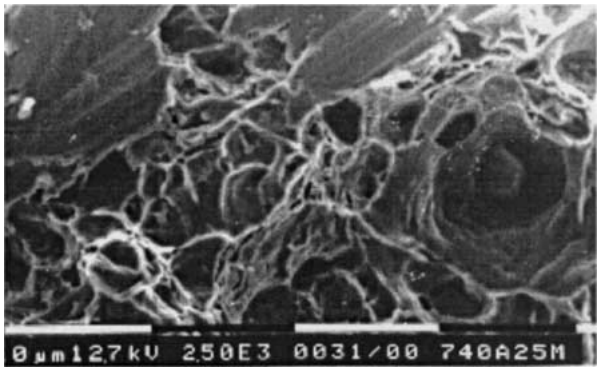

Figure 15 Fracture surface with ductile dimples and cleavage facets in 740A25.

or elliptical depending on the stress state [33]. This type of fracture surface arises because microvoids are initiated at second phase particles during deformation. The voids grow and eventually the ligaments between the microvoids fracture by ductile necking to knife-edges. In other samples of Series A and B, cleavage facets were not observed. This suggests that the critical stress for cleavage had not been achieved in the ferrite at the moment of final fracture. Possible this is due to the low martensite content of the samples.

Kim and Thomas [34] observed that in fracture of coarse dual phase microstructure, the critical stress for cleavage had not been achieved in the ferrite at the moment of final fracture. Cleavage fracture [33] is a low energy, brittle fracture which propagates along low index crystallographic planes. This fracture is characterised by flat, cleavage facets, which are generally about the size of a ferrite grain in the case of steels. River markings on the facets result from the propagation of the crack on a number of planes of different levels.

He *et al*. [32] reported that the fracture mode of the completely failed surface consisted of a central region, formed by the growth and coalescence of voids, and a brittle, cleavage-type of fracture of the remaining section. In the fine structure, microvoids initiated by decohesion of the interface between martensite and ferrite and failure occurred by the classical, ductile 'cup and cone' process occurred in the early stage of deformation by cleavage crack initiation in martensite and propagation in the ferrite matrix.

In C-Mn-Si-Cr microalloyed steels of dual phase microstructure having different volume fractions of martensite, Uggowitzer and Stuwe [26]. observed both ductile dimples and cleavage facets, depending on the volume fraction of martensite. In this work voids nucleated by decohesion at interfaces between ferrite and martensite, at sulphide particles and by cracking of sulphides. Decohesion at martensite-ferrite interfaces occurred only when sulphide particles were present in the interface.

6. Conclusions

1. New ferrite is an identifiable, controllable parameter and influences tensile fracture behaviour in microalloyed dual phase steels. At constant volume percent martensite microvoids density increases with increasing new ferrite content.

2. The new ferrite is more effective in fine dual phase microstructures than coarse ones concerning the tensile properties of dual phase steels.

3. In both fine and coarse dual phase structures microvoids formed at martensite particles, inclusions and martensite-ferrite interfaces in the necked region.

4. Martensite morphology had an influence in determining martensite cracking. Coarse and interconnected martensite distributed along ferrite grain boundaries cracked easily.

5. Martensite cracking was less frequent and the microvoids were smaller in the fine structure than the coarse structure. Microvoid coalescence was the dominant form of fracture in both structures.

Acknowledgement

I would like to thank Dr. R. Priestner for his invaluable discussion.

References

1. R. G. DAVIES, in "Formable HSLA and Dual Phase Steels," edited by A. T. Davenport (AIME, New York, 1979) p. 25.
2. J. Y. KOO and G. THOMAS, in "Formable HSLA and Dual Phase Steels," edited by A. T. Davenport (AIME, New York, 1979) p. 40.
3. R. D. LAWSON, D. K. MATLOCK and G. KRAUSS, in "Fundamentals of Dual Phase Steels," edited by R. A Kot and B. L. Bramfitt (AIME, New York, 1981) p. 347.
4. S. S. HANSEN and R. R. PRADHAN, in "Structure and Properties of Dual Phase Steels," edited by R. A. Kott and J. W. Morris (AIME, New York, 1979) p. 91.
5. R. G. DAVIES, *Met. Trans*. **9A** (1978) 671.
6. *Idem.*, *ibid*. **10A** (1979) 1549.
7. A. R. MARDER, in "Formable HSLA and Dual Phase Steels," edited by A. T. Davenport (AIME, New York, 1979) p. 87.
8. X. L. CAI, J. FENG and W. S. OWEN, *Met. Trans*. **11A** (1980) 1683.
9. X. J. HE, N. TERAO and A. BERGHEZAN, *J. Mater. Sci*. **18** (1984) 367.
10. Y. TOMOTA, *Mat. Sci and Tech*. **3** (1987) 415.
11. M. ERDOGAN and S. TEKELI, in "International Conference on Advances in Materials and Processing Technologies," September 2001, edited by J. M Torralba, Leganes, Madrid, Spain, p. 117.
12. M. ERDOGAN, S. TEKELI, O. PAMUK and A. ERKAN, *Mat. Sci. and Tech*., in press.
13. G. KRAUSS and A. R. MARDER, *Met. Trans*. **2A** (1971) 2343.
14. T. JURUKUWA, H. MORIKAWA, H. TAKECHI and K. KOYAMA, in "Structure and Properties of Dual Phase Steels," edited by R. A. Kott and J. W. Morris (AIME, New York, 1979) p. 281.
15. G. S. HUPPI, D. K. MATLOCK and G. KRAUSS, *Scrip. Metall* **14** (1980) 1239.

16. M. ERDOGAN and R. PRIESTNER, *Mat. Sci. and Tech*. **15** (1999) 1273.
17. *Idem.*, *ibid*. **18** (2002) 369.
18. E. ROBERT and D. REED-HILL, in "Physical Metallurgy Principles" (Van Nostrand, New York, 1973).
19. M. COSTER and J. L. CHESMONT, *Int. Met. Rev*. **28** (1983) 228.
20. R. D. LAWSON, D. K. MATLOCK and G. KRAUSS, *Metallography* **13** (1980) 71.
21. B. D. CULLITY, in "Elements of X-Ray Diffraction" (MMA, Addison-Wesley, USA, 1978) p. 411.
22. L. STEINBRUNNER, D. K. MATLOCK and G. KRAUSS, *Met. Trans*. **19A** (1988) 579.
23. S. RASHID, in "Formable HSLA and Dual Phase Steels," edited by A. T. Davenport (AIME, New York, 1979) p. 1.
24. G. THOMAS and Y. J. KOO, in "Fundamentals of Dual Phase Steels," edited by R. A. Kot and B. L. Bramfitt (AIME, New York, 1981) p. 183.
25. M. D. GEIB, D. K. MATLOCK and G. KRAUSS, *Met. Trans*. **11A** (1980) 1683.
26. P. UGGOWITZER and H. P. STUWE, *Mat. Sci. and Eng*. **55** (1982) 181.
27. A. H. NAKAGAWA and G. THOMAS, *Met. Trans*. **16A** (1985) 831.
28. M. SARWAR and R. PRIESTNER, *J. Mater. Sci.* **31** (1996) 2091.
29. E. AHMAD, T. MANZOROR, K. L. ALI and J. I. AKHAR, *Mat. Eng. and Per*. **9** (2000) 306.
30. G. R. SPEICH and R. L. MILLER, in "Structure and Properties of Dual Phase Steels," edited by R. A. Kott and J. W. Morris (AIME, New York, 1979) p. 145.
31. N. K. BALLIGER, in "Advances in the Physical Metallurgy and Application of Steel" (The Metal Society, London, 1982) p. 73.
32. X. J. HE, N. TERAO and A. BERGHEZAN, *J. Mater. Sci*. **18** (1984) 367.
33. G. E. DIETER, in "Mechanical Metallurgy" (McGraw Hill Co., New York, 1986).
34. N. J. KIM and G. THOMAS, *Met. Trans*. **12A** (1981) 483.

Received 27 September 2001
and accepted 10 April 2002